

Modeling and simulation of A Single-Stage PFC Half-Bridge Converter by using PMBLDCM Drive

¹K.PrabhakaraRao, ²A.Venkatraman, ³K.Saiteja,

^{1,2,3,4} Assistant Professor

¹Electrical and Electronics Engineering Department,
¹Dvr&Dr Hs Mic College of Technology , Vijayawada, India

Abstract — In this paper, a buck half-bridge DC-DC converter is used as a single-stage power factor correction (PFC) converter for feeding a voltage source inverter (VSI) based permanent magnet brushless DC motor (PMBLDCM) drive. The front end of this PFC converter is a diode bridge rectifier (DBR) fed from single-phase AC mains. The PMBLDCM is used to drive a compressor load of an air conditioner through a three-phase VSI fed from a controlled DC link voltage. The speed of the compressor is controlled to achieve energy conservation using a concept of the voltage control at DC link proportional to the desired speed of the PMBLDCM. Therefore the VSI is operated only as an electronic commutator of the PMBLDCM. The stator current of the PMBLDCM during step change of reference speed is controlled by a rate limiter for the reference voltage at DC link. The proposed PMBLDCM drive with voltage control based PFC converter is designed, modeled and its performance is simulated in Matlab-Simulink environment for an air conditioner compressor driven through a 2 kW, 1500 rpm PMBLDC motor. The evaluation results of the proposed speed control scheme are presented to demonstrate an improved efficiency of the proposed drive system with PFC feature in wide range of the speed and an input AC voltage.

Index Terms—Buck Half-bridge converter, Voltage control, Power Factor Correction (PFC), Voltage Source Inverter (VSI), Permanent Magnet Brushless DC Motor (PMBLDCM), Mat lab- Simulink,

I. INTRODUCTION

PERMANENT magnet brushless DC motors (PMBLDCMs) are preferred motors for a compressor of an air-conditioning system due to its features like high efficiency, low maintenance requirements and wide speed range. The operation of the compressor with the speed control results in an improved efficiency of the system while maintaining the temperature in the air-conditioned zone at the set reference consistently. Whereas, the existing air conditioners mostly have a single-phase induction motor to drive the compressor in 'ON/OFF' control mode.

A PMBLDCM which is a kind of three-phase synchronous motor with permanent magnets (PMs) on the rotor and trapezoidal back EMF waveform operates on electronic commutation accomplished by solid state switches. It is powered through a three-phase voltage source inverter (VSI) which is fed from single-phase AC supply using a diode bridge rectifier (DBR) followed by smoothening DC link capacitor. The compressor exerts constant torque on the PMBLDCM and is operated in speed control mode to improve the efficiency of the Air-Con system. Since, the back-emf of the PMBLDCM is proportional to the motor speed and the developed torque is proportional to its phase current [1-4], therefore, a constant torque is maintained by a constant current in the stator winding of the PMBLDCM whereas the speed can be controlled by varying the terminal voltage of the motor.

The PMBLDCM drive, fed from a single-phase AC mains through a diode bridge rectifier (DBR) followed by a DC link capacitor, suffers from power quality disturbances such as poor power factor, increased total harmonic distortion (THD) of current at input AC mains and its high crest factor. It is mainly due to uncontrolled charging of the DC link capacitor which results in a pulsed current waveform having a peak value higher than the amplitude of the fundamental input current at AC mains.

For these applications, the brushless dc motor offers the following advantages: small size, reliability, no carbon dust from brushes, precise speed control, and potentially high efficiency. Reliability and controllability are the two major factors for industrial based motors. These can be achieved through proper choice of controllers. The construction of modern Brushless Motors is very similar to the AC motor, known as the Permanent Magnet Synchronous Motor. The stator windings are similar to those in a Poly-Phase AC motor. Although it is said that Brushless DC motors and Conventional DC motors are similar in their static characteristics they actually have remarkable differences in some aspects. In a Conventional DC motors commutation is undertaken by brushes and commutator in contrast, in a Brushless DC motor it is done by using semiconductor devices such as transistor. The control of BLDC motor can be done in sensor or sensor less mode [8], the most common position/pole sensor in the hall element, but some motors use optical sensors. Coming to sensorless, to reduce overall cost of actuating devices, these control techniques are normally used. A detailed modeling, design and performance evaluation of the proposed drive are presented for an air conditioner compressor driven by a PMBLDC motor of 1.5 kW, 1500 rpm rating.

II. PROPOSED SPEED CONTROL SCHEME OF PMBLDC MOTOR FOR AIR CONDITIONER

The proposed speed control scheme as shown in Fig. 1 controls reference voltage at DC link as an equivalent reference speed, thereby replaces the conventional control of the motor speed and a stator current involving various sensors for voltage and current signals. Therefore, rotor-position information is required only at the commutation points, e.g., every 60° electrical in the three-phase. The rotor position of PMBLDCM is sensed using Hall effect position sensors and used to generate switching sequence for the VSI as shown in Table-I.

The PFC control scheme uses a current control loop inside the speed control loop with current multiplier approach which operates in continuous conduction mode (CCM) with average current control. The control loop begins with the comparison of sensed DC link voltage with a voltage equivalent to the reference speed. This signal is multiplied with a unit template of input AC voltage and compared with DC current sensed after the DBR. For the current control of the PMBLDCM during step change of the reference voltage due to the change in the reference speed, a voltage gradient less than 800 V/s is introduced for the change of DC link voltage, which ensures the stator current of the PMBLDCM within the specified limits (i.e. double the rated current).

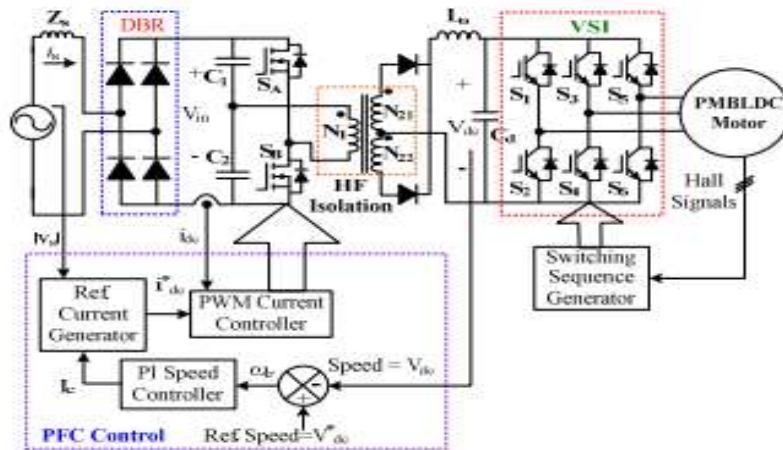


Figure 1. Schematic Control of Proposed Bridge-buck PFC converter fed PMBLDCM drive

III. DESIGN OF PFC BUCK HALF-BRIDGE CONVERTER BASED PMBLDCM DRIVE

The proposed PFC buck half-bridge converter is designed for a PMBLDCM drive with main considerations on PQ Constraints at AC mains and allowable ripple in DC link voltage. The DC link voltage of the PFC converter is given as,

$$V_{dc} = 2(N_2/N_1)V_{in}D \text{ and } N_2 = N_{21} = N_{22} \quad (1)$$

where N_1 , N_{21} , N_{22} are number of turns in primary, secondary upper and lower windings of the high frequency (HF) isolation transformer, respectively. V_{in} is the average output of the DBR for a given AC input voltage (V_s) related as,

$$V_{in} = \frac{2\sqrt{2}V_s}{\pi} \quad (2)$$

The output filter inductor and capacitor are given as,

$$L_0 = (0.5-D)V_{dc}/\{f_s(I_{L0})\} \quad (3)$$

The PFC converter designed based on DC link voltage of $V_{dc}=400V$ at $V_{in}=220V_{rms}$. turns ratio of HFT is 6:1 to maintain desired DC link voltage at low input AC voltages typically at 170V. $f_s=40$ KHz, $I_o=4A$, $V_{cd}=4V$ (1% of V_{dc}), $I_{L0}=0.8$ A (20% of I_o). The design parameters are calculated as $L_0=2.0$ mH, $C_d=1600$ μF

$$C_d = I_o / (2\omega \Delta V_{Cd}) \quad (4)$$

TABLE 1. Shows the Hall Effect Sensor Signal Based on VSI

H_a	H_b	H_c	E_a	E_b	E_c	S_1	S_2	S_3	S_4	S_5	S_6
0	0	0	0	0	0	0	0	0	0	0	0
0	0	1	0	-1	+1	0	0	0	1	1	0
0	1	0	-1	+1	0	0	1	1	0	0	0
0	1	1	-1	0	+1	0	1	0	0	1	0
1	0	0	+1	0	-1	1	0	0	0	0	1
1	0	1	+1	-1	0	1	0	0	1	0	0
1	1	0	0	+1	-1	0	0	1	0	0	1
1	1	1	0	0	0	0	0	0	0	0	0

IV. MODELING OF THE PROPOSED PMBLDCM DRIVE

The main components of the proposed PMBLDCM drive are the PFC converter and PMBLDCM drive, which are modeled by mathematical equations and the complete drive is represented as a combination of these models.

A. *PFC Converter* :The modeling of the PFC converter consists of the modeling of a speed controller, a reference current generator and a PWM controller as given below.

Speed Controller: The speed controller, the prime component of this control scheme, is a proportional-integral

(PI) controller which closely tracks the reference speed as an equivalent reference voltage. If at k^{th} instant of time, $V_{dc}^*(k)$ is reference DC link voltage, $V_{dc}(k)$ is sensed DC link voltage then the voltage error $V_e(k)$ is calculated as the PI controller gives desired control signal after processing this voltage error. The output of the controller $I_c(k)$ at k^{th} instant is given as, Reference Current Generator: The reference input current of the PFC converter is denoted by i_{dc}^* and given as,

$$i_{dc}^* = I_c(k) uVs \tag{5}$$

Where uVs is the unit template of the voltage at input AC mains, calculated as,

$$uVs = vd/Vsm; vd = |vs|; vs = Vsm \sin \omega t \tag{6}$$

Where Vsm is the amplitude of the voltage and ω is frequency in rad/sec at AC mains.

PWM Controller: The reference input current of the buck half-bridge converter (i_{dc}^*) is compared with its sensed Current (i_{dc}) to generate the current error $i_{dc} = (i_{dc}^* - i_{dc})$. This current error is amplified by gain k_{dc} and compared with fixed Frequency (f_s) saw-tooth carrier waveform $md(t)$ (as shown in Fig.2) in unipolar switching mode [7] to get the switching Signals for the MOSFETs of the PFC buck half-bridge converter as

$$I_c(k) = I_c(k-1) + K_p \{V_e(k) - V_e(k-1)\} + K_i V_e(k) \tag{7}$$

Where K_p and K_i are the proportional and integral gains of the PI controller.

$$\text{If } -k_{dc}i_{dc} > md(t) \text{ then } S_B = 1 \text{ else } S_B = 0 \tag{8}$$

where S_A, S_B are upper and lower switches of the half-bridge converter as shown in Fig. 1 and their values '1' and '0' represent 'on' and 'off' position of the respective MOSFET of the PFC converter.

B.PMBLDCM Drive

The PMBLDCM drive consists of an electronic commutator, a VSI and a PMBLDC motor.

1) Electronic Commutator: The electronic commutator uses signals from Hall effect position sensors to generate the switching sequence for the voltage source inverter based on the logic given in Table I.

2) Voltage Source Inverter: Fig. 3 shows an equivalent circuit of a VSI fed PMBLDCM. The output of VSI to be fed to phase 'a' of the PMBLDC motor is given as,

$$v_{ao} = (V_{dc}/2) \text{ for } S_1 = 1 \tag{9}$$

$$v_{ao} = (-V_{dc}/2) \text{ for } S_2 = 1 \tag{10}$$

$$v_{ao} = 0 \text{ for } S_1 = 0, \text{ and } S_2 = 0 \tag{11}$$

$$v_{an} = v_{ao} - v_{no} \tag{12}$$

where v_{ao}, v_{bo}, v_{co} , and v_{no} are voltages of the three-phases and neutral point (n) with respect to virtual mid-point of the DC link voltage shown as 'o' in Fig. 3. The voltages v_{an}, v_{bn}, v_{cn} are voltages of three-phases with respect to neutral point (n) and V_{dc} is the DC link voltage. $S = 1$ and 0 represent 'on' and 'off' position of respective IGBTs of the VSI and considered in a similar way for other IGBTs of the VSI i.e. $S_3 - S_6$. Using similar logic $v_{bo}, v_{co}, v_{bn}, v_{cn}$ are generated for other two phases of the VSI feeding PMBLDC motor.

3) PMBLDC Motor: The PMBLDCM is represented in the form of a set of differential equations [3] given as,

$$v_{an} = R i_a + p \lambda_a + e_{an} \tag{13}$$

$$v_{bn} = R i_b + p \lambda_b + e_{bn} \tag{14}$$

$$v_{cn} = R i_c + p \lambda_c + e_{cn} \tag{15}$$

where p is a differential operator (d/dt), i_a, i_b, i_c are three-phase currents, $\lambda_a, \lambda_b, \lambda_c$ are flux linkages and e_{an}, e_{bn}, e_{cn} are phase to neutral back emfs of PMBLDCM, in respective phases, R is resistance of motor windings/phase.

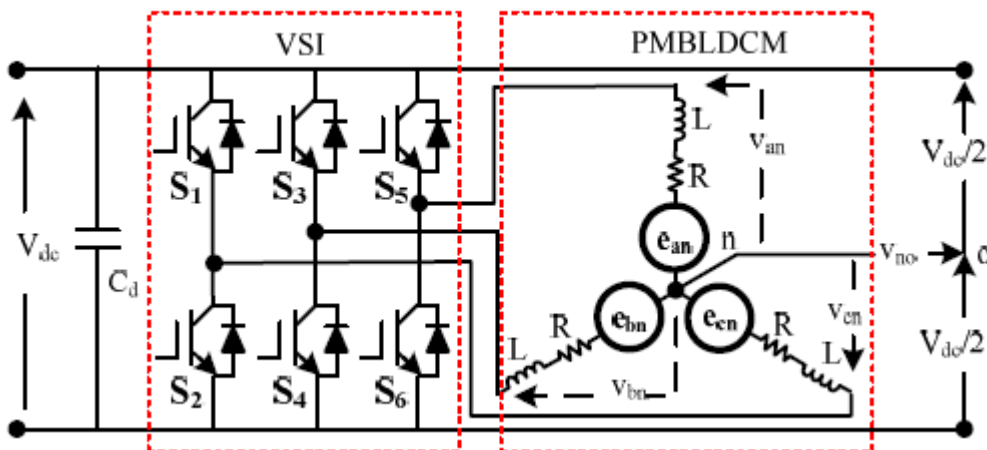


Figure 3. Equivalent Circuit of a VSI fed PMBLDCM Drive

The flux linkages are represented as,

$$\lambda_a = L i_a - M (i_b + i_c) \quad (16)$$

$$\lambda_b = L i_b - M (i_a + i_c) \quad (17)$$

$$\lambda_c = L i_c - M (i_b + i_a) \quad (18)$$

where L is self-inductance/phase, M is mutual inductance of motor winding/phase. Since the PMBLDCM has no neutral connection, therefore,

$$i_a + i_b + i_c = 0 \quad (19)$$

From Eqs. (14-21) the voltage between neutral terminal (n) and mid-point of the DC link (o) is given as,

$$v_{no} = \{v_{ao} + v_{bo} + v_{co} - (e_{an} + e_{bn} + e_{cn})\}/3 \quad (20)$$

From Eqs. (18-21), the flux linkages are given as,

$$\lambda_a = (L+M) i_a, \lambda_b = (L+M) i_b, \lambda_c = (L+M) i_c, \quad (21)$$

From Eqs. (15-17 and 23), the current derivatives in generalized state space form are given as,

$$p i_x = (v_{xn} - i_x R - e_{xn})/(L+M) \quad (22)$$

where x represents phase a, b or c. The developed electromagnetic torque T_e in the PMBLDCM is given as,

$$T_e = (e_{an} i_a + e_{bn} i_b + e_{cn} i_c)/\omega \quad (23)$$

where ω is motor speed in rad/sec,

The back emfs may be expressed as a function of rotor position (θ) as,

$$e_{xn} = K_b f_x(\theta) \omega \quad (24)$$

where x can be phase a, b or c and accordingly $f_x(\theta)$ represents function of rotor position with a maximum value ± 1 , identical to trapezoidal induced emf given as,

$$f_a(\theta) = 1 \text{ for } 0 < \theta < 2\pi/3 \quad (25)$$

$$f_a(\theta) = \{(6/\pi)(\pi - \theta)\} - 1 \text{ for } 2\pi/3 < \theta < \pi \quad (26)$$

$$f_a(\theta) = -1 \text{ for } \pi < \theta < 5\pi/3 \quad (27)$$

$$f_a(\theta) = \{(6/\pi)(\theta - 2\pi)\} + 1 \text{ for } 5\pi/3 < \theta < 2\pi \quad (28)$$

The functions $f_b(\theta)$ and $f_c(\theta)$ are similar to $f_a(\theta)$ with a phase difference of 120° and 240° respectively. Therefore, the electromagnetic torque is expressed as,

$$T_e = K_b \{f_a(\theta) i_a + f_b(\theta) i_b + f_c(\theta) i_c\} \quad (29)$$

The mechanical equation of motion in speed derivative form is given as,

$$p\omega = (P/2) (T_e - T_L - B\omega)/(J) \quad (30)$$

The derivative of the rotor position angle is given as,

$$p\theta = \omega \quad (31)$$

where P is no. poles, TL is load torque in Nm, J is moment of inertia in kg-m² and B is friction coefficient in Nms/Rad.

V. PERFORMANCE EVALUATION OF PROPOSED PFC DRIVE

The proposed PMBLDCM drive is modeled in Matlab-Simulink environment and evaluated for an air conditioning compressor load. The performance of the proposed PFC drive is evaluated on the basis of various parameters such as total harmonic distortion (THDi) and the crest factor (CF) of the current at input AC mains, displacement power factor (DPF), power factor (PF) and efficiency of the drive system (η_{drive}) at different speeds of the motor. Moreover, these parameters are also evaluated for variable input AC voltage at DC link voltage of 416 V which is equivalent to the rated speed (1500 rpm) of the PMBLDCM.

A. Performance during Starting

The performance of the proposed PMBLDCM drive fed from 220 V AC mains during starting at rated torque and 900rpm speed. A rate limiter of 800 V/s is introduced in the reference voltage to limit the starting current of the motor as well as the charging current of the DC link capacitor. The current (i_s) waveform at input AC mains is in phase with the supply voltage (v_s) demonstrating nearly unity power factor during the starting.

B. Performance under Speed Control Figs. 4-6 show the performance of the proposed PMBLDCM drive under the speed control at constant rated torque (9.55 Nm) and 220 V AC mains supply voltage. These results are categorized as performance during transient and steady state conditions.

1) Transient Condition: the performance of the drive during the speed control of the compressor. The reference speed is changed from 900 rpm to 1500 rpm for the rated load performance of the compressor; from 900 rpm to 300 rpm for performance of the compressor at light load. It is observed that the speed control is fast and smooth in either direction i.e. acceleration or retardation with power factor maintained at nearly unity value.

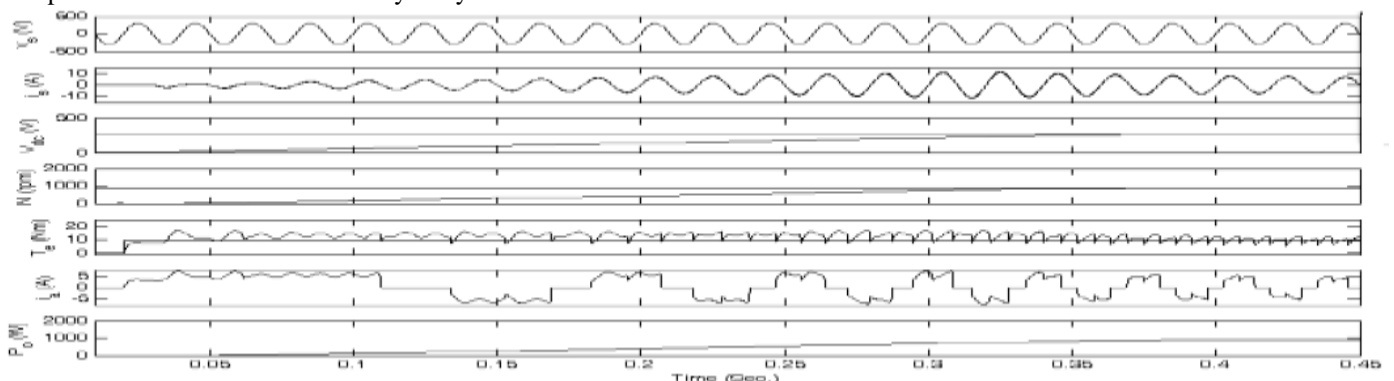


Fig. 4a: Starting performance of the PMBLDCM drive at 900 rpm.

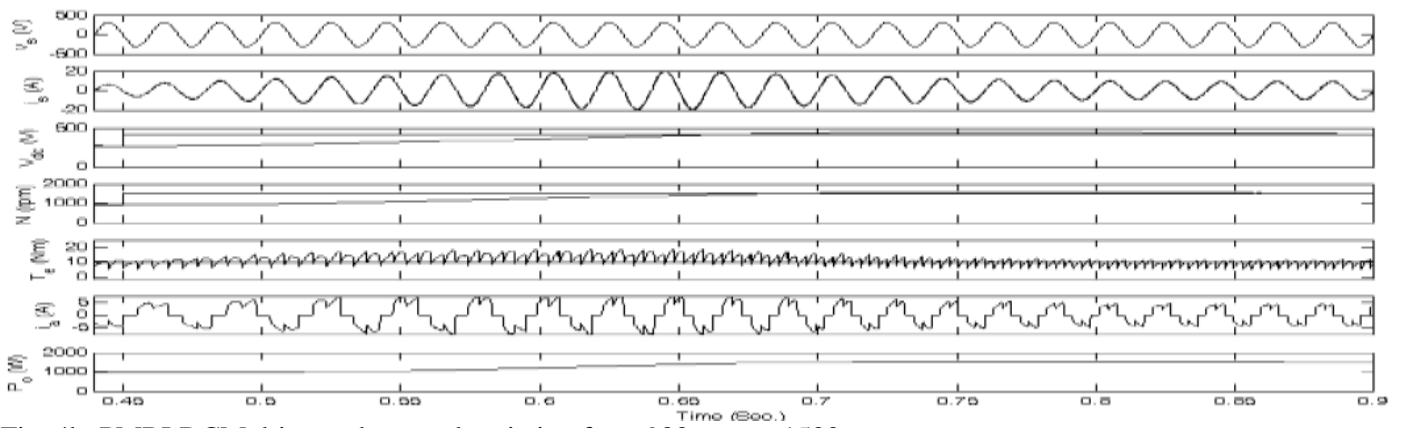


Fig. 4b: PMBLDCM drive under speed variation from 900 rpm to 1500 rpm.

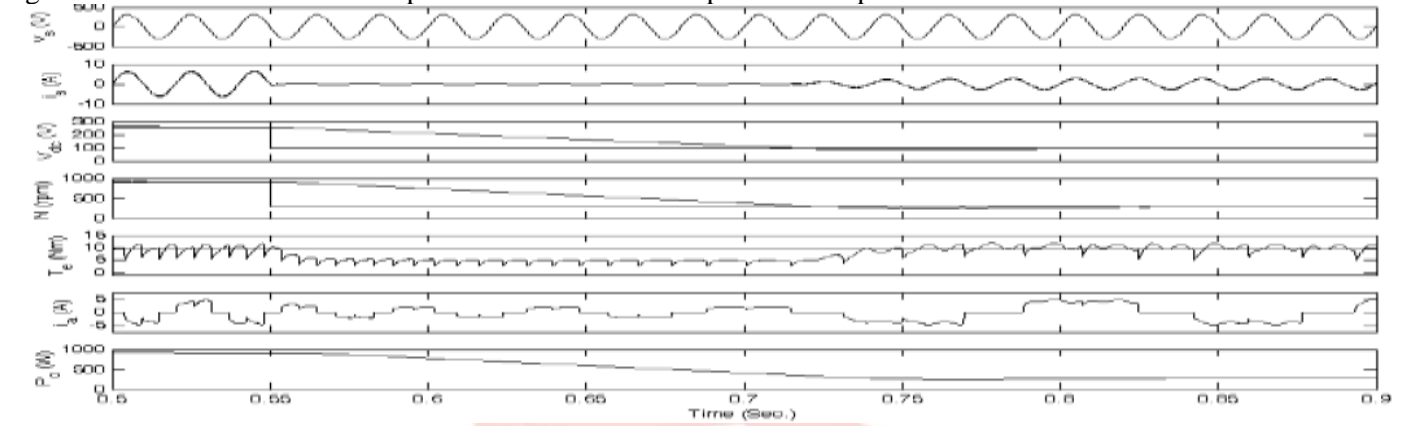


Fig. 4c: PMBLDCM drive under speed variation from 900 rpm to 300 rpm.

Figure 4. Performance of the Proposed PMBLDCM drive under speed variation at 220 VAC input.

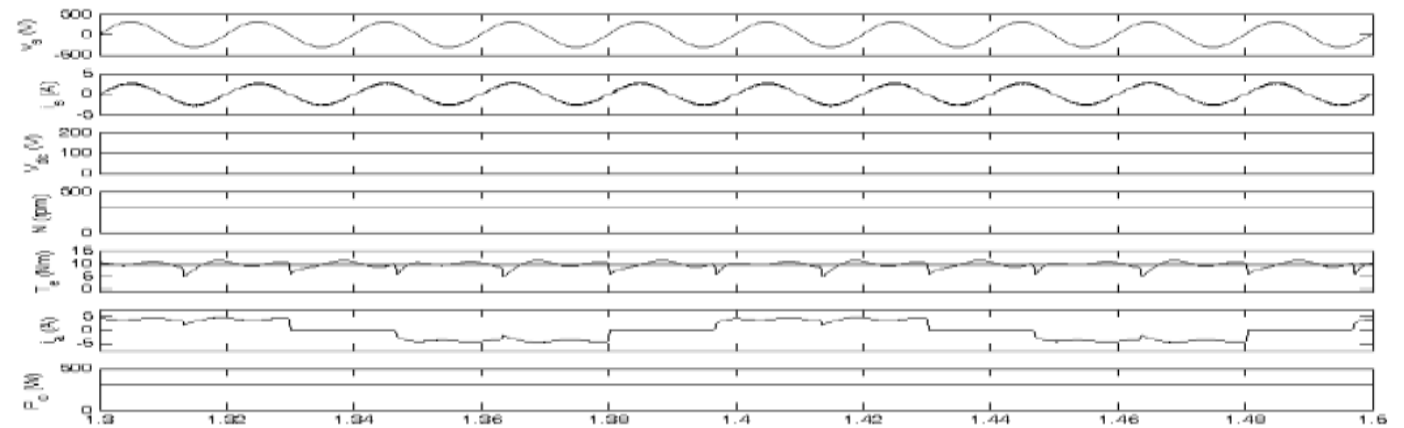


Fig. 5a: Performance of the PMBLDCM drive at 300 rpm.

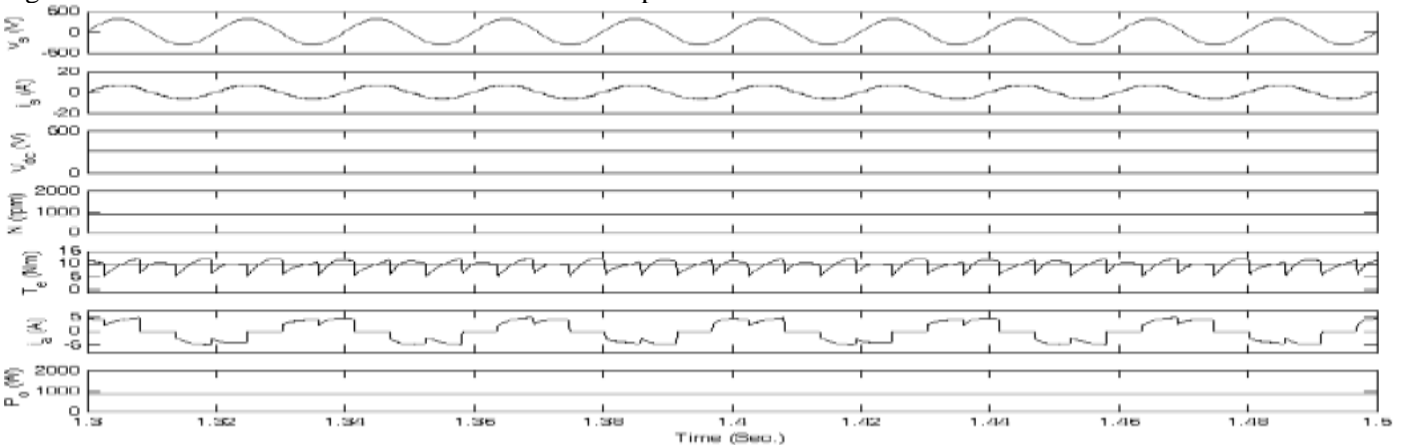


Fig. 5b: Performance of the PMBLDCM drive at 900 rpm.

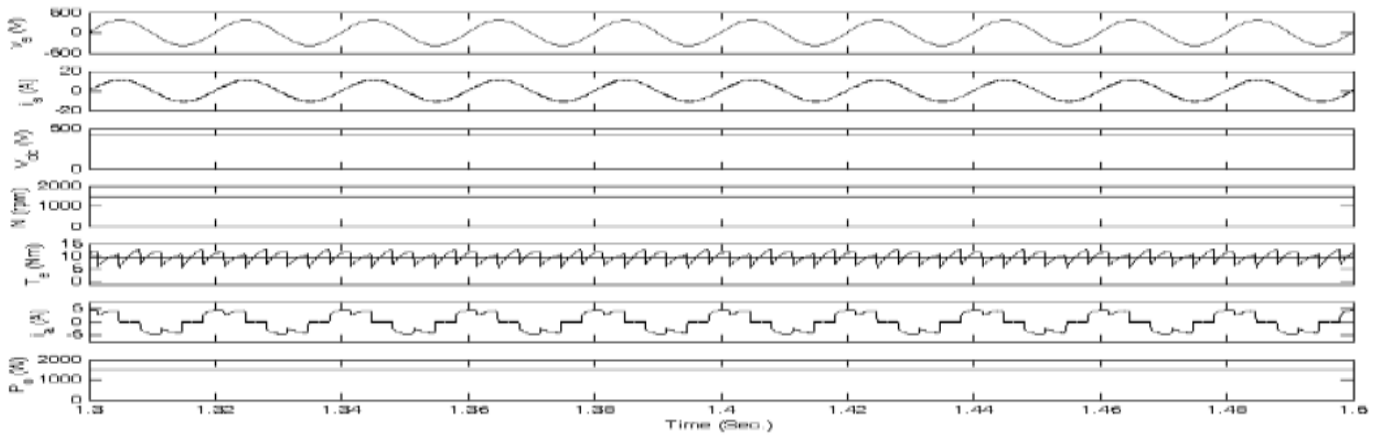


Fig. 5c: Performance of the PMBLDCM drive at rated speed (1500 rpm).

Figure 5. Performance of the PMBLDCM drive under steady state condition at 220 VAC input.

Steady State Condition: The speed control of the PMBLDCM driven compressor under steady state condition is carried out for different speeds and the results are shown in Figs. 5-6 and Table-II to demonstrate the effectiveness of the proposed drive in wide speed range. Figs. 5a-c show voltage (vs) and current (is) waveforms at AC mains, DC link voltage (Vdc), speed of the motor (N), developed electromagnetic torque of the motor (Te), the stator current of the PMBLDC motor for phase ‘a’ (Ia), and shaft power output (Po) at 300 rpm, 900 rpm and 1500 rpm speeds. Fig. 6a shows linear relation between motor speed and DC link voltage. Since the reference speed is decided by the reference voltage at DC link, it is observed that the control of the reference DC link voltage controls the speed of the motor instantaneously.

C. Power Quality Performance The performance of the proposed PMBLDCM drive in terms of various PQ parameters such as THDi, CF, DPF, PF is summarized in Table-II and shown in Figs. 7-8. Nearly unity power factor (PF) and reduced THD of AC mains current are observed in wide speed range of the PMBLDCM as shown in Figs. 7a-b. The THD of AC mains current remains less than 5% along with nearly unity PF in wide range of speed as well as load as shown in Table-II and Figs. 8a-c.

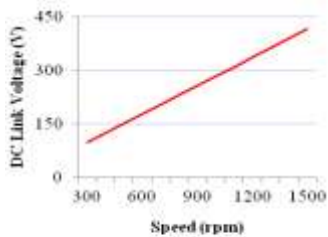


Fig. 6a. DC link voltage with speed

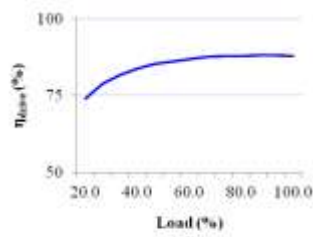


Fig. 6b. Efficiency with load

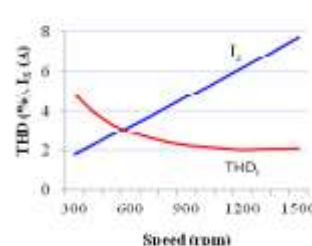


Fig. 7a. THD of current at AC mains

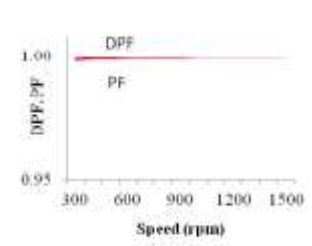


Fig. 7b. DPF and PF

Figure 6. Performance of the proposed PFC drive under speed control at rated torque and 220 V_{AC}

Figure 7. PQ parameters of PMBLDCM drive under speed control at rated torque and 220 V_{AC} input

TABLE II. PERFORMANCE OF DRIVE UNDER SPEED CONTROL AT 220 V SUPPLY

Speed (rpm)	VDC (V)	THDi (%)	DPF	PF	ηdrive (%)	Load (%)
400	100	4.79	0.99	0.99	80	26.3
600	180	3.96	0.99	0.99	81.1	40.0
800	232	3.30	0.99	0.99	86.3	52.9
900	261	2.26	0.99	0.99	86.9	59.6
1000	285	2.18	0.99	0.99	87.5	67.1
1200	340	2.03	0.99	0.99	88.2	80.0
1400	389	2.02	0.99	0.99	88.8	94.2
1500	415	2.01	0.99	0.99	89.0	100

D. Performance under Variable Input AC Voltage Performance evaluation of the proposed PMBLDCM drive is carried out under varying input AC voltage at rated load (i.e. rated torque and rated speed) to demonstrate the operation of proposed PMBLDCM drive for air conditioning system in various practical situations as summarized in Table-III. Figs. 9a-b show variation of input current and its THD at AC mains, DPF and PF with AC input voltage. The THD of current at AC mains is within specified limits of international norms along with nearly unity power factor in wide range of AC input voltage.

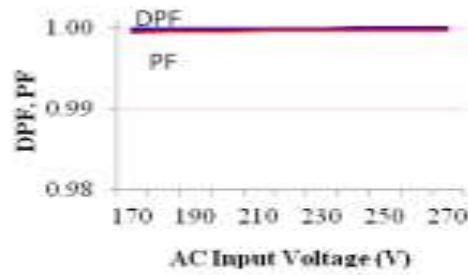
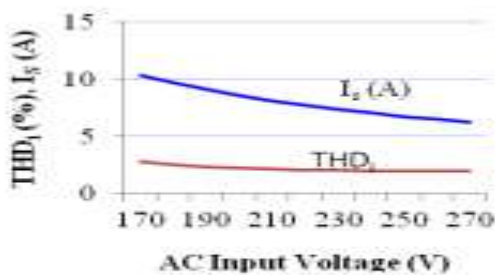


Fig. 9a. Current at AC mains and its THD

Fig. 9b. DPF and PF

Figure 9. PQ parameters with input AC voltage at 416 V_{DC} (1500 rpm)

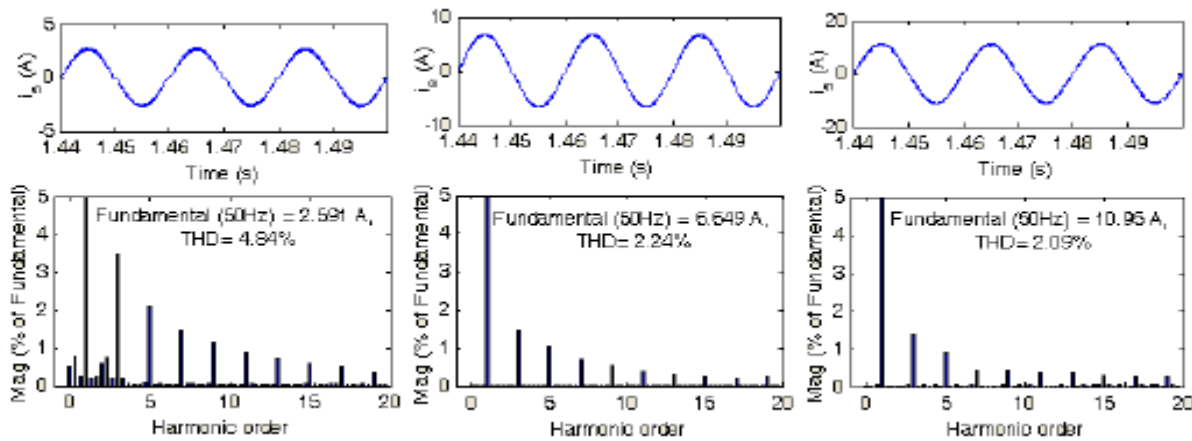


Fig. 8a. At 300 rpm

Fig. 8b. At 900 rpm

Fig. 8c. At 1500 rpm

Figure 8. Current waveform at AC mains and its harmonic spectra of the PMBLDCM drive under steady state condition at rated torque and 220 VA

Vac (V)	THDi (%)	DPF	PF	CF	Ia(A)	η_{drive} (%)
170	2.87	0.99	0.9995	1.41	10.3	84
180	2.58	0.99	0.9996	1.41	9.7	85
190	2.39	0.99	0.9996	1.41	9.2	86
200	2.28	0.99	0.9997	1.41	8.6	87
210	2.16	0.99	0.9997	1.41	8.2	88
220	2.11	0.99	0.9997	1.41	7.7	88
230	2.06	0.99	0.9998	1.41	7.4	89

VI. CONCLUSION

The speed control strategy of a PMBLDCM drive is validated for a compressor load of an air conditioner which uses the reference speed as an equivalent reference voltage at DC link. The speed control is directly proportional to the voltage control at DC link. The rate limiter introduced in the reference voltage at DC link effectively limits the motor current within the desired value during the transient condition (starting and speed control). The additional PFC feature to the proposed drive ensures nearly unity PF in wide range of speed and input AC voltage. As the load torque varies the speed of the BLDC motor remains constant. The mathematical modeling of BLDC motor is done and the speed control of the BLDC motor by using permanent magnet brushless DC motor (PMBLDCM) drive. The proposed drive has demonstrated good speed control with energy efficient operation of the drive system in the wide range of speed and input AC voltage. The proposed drive has been found as a promising candidate for a PMBLDCM driving Air-Con load in 1-2 kW power range.

APPENDIX Rated Power: 1.5 kW, rated speed: 1500 rpm, rated current: 4.0 A, rated torque: 9.55 Nm, number of poles: 4, stator resistance (R): 2.8 Ω /ph., inductance (L+M): 5.21 mH/ph., back EMF constant (Kb): 0.615 Vsec/rad, inertia (J): 0.013 Kg-m². Source impedance (Zs): 0.03 pu, switching frequency of PFC switch (fs) = 40 kHz, capacitors (C1= C2): 15nF, PI speed controller gains (Kp): 0.145, (Ki): 1.45.

REFERENCES

[1] Vandana Govindan T.K, Anish Gopinath and S. Thomas. 2011. George 'DSP based Speed control of Permanent Magnet Brushless DC motor. IJCA Special Issue on Computational Science - New Dimensions and Perspectives NCCSE.

- [2] Cheng-Tsung Lin, Chung-Wen Hung and Chih-Wen Liu. 2007. Fuzzy PI controller for BLDC motors considering Variable Sampling Effect. IEEE Industrial Electronics Society (IECON). Nov. 5-8, Taipei, Taiwan.
- [3] J. R. Hendershort and T. J. E. Miller, *Design of Brushless Permanent- Magnet Motors*, Clarendon Press, Oxford, 1994.
- [4] Ji Hun, Li Zhiyong. 2008. Simulation of Sensorless Permanent magnetic brushless DC motor control System. Proceedings othe IEEE International conference on automation and logistics. September, Quigdao, China.
- [5] Limits for Harmonic Current Emissions (Equipment input current $\leq 16A$ per phase), Internationa Standard IEC 61000-3-2, 2000.
- [6] B. Singh, B. N. Singh, A. Chandra, K. Al-Haddad, A. Pandey and D. P. Kothari, "A review of single-phase improved power quality AC-DC converters," *IEEE Trans. Industrial Electron.*, vol. 50, no. 5, pp. 962 – 981, oct. 2003.
- [7] N. Mohan, T. M. Undeland and W. P. Robbins, "*Power Electronics: Converters, Applications and Design*," John Wiley, USA, 1995.
- [8] A. I. Pressman, *Switching Power Supply Design*, McGraw Hill, New York, 1998.
- [9] P. Pillay and R. krrishnan. 2002. Modelling simulation and analysis of a Permanent magnet brushless Dc motor drive. IEEE trans. Ind Applicant. 26: 124-129.
- [10] J.Y. Lee, G.W. Moon and M.J. Youn, "Design of a power-factorcorrection converter based on half-bridge topology," *IEEE Trans. Ind. Electron.*, vol. 46, no. 4, pp.710 – 723, Aug 1999.
- [11] J. Sebastian, A. Fernandez, P.J. Villegas, M.M. Hernando and J.M. Lopera, "Improved active input current shapers for converters with symmetrically driven transformer," *IEEE Trans. Ind. Appl.*, vol. 37, no. 2, pp. 592 – 600, March-April 2001.
- [12] A. Fernandez, J. Sebastian, M.M. Hernando and P. Villegas, "Small signal modelling of a half bridge converter with an active input current shaper," in *Proc. IEEE PESC*, 2002, vol.1, pp.159 – 164.
- [13] S.K. Han, H.K. Yoon, G.W. Moon, M.J. Youn, Y.H. Kim and K.H. Lee, "A new active clamping zero-voltage switching PWM current-fed half-bridge converter," *IEEE Trans. Power Electron.*, vol. 20, no. 6, pp. 1271 – 1279, Nov. 2005.
- [14] R.T.Bascope, L.D.Bezerra, G.V.T.Bascope, D.S. Oliveira, C.G.C. Branco, and L.H.C. Barreto, "High frequency isolation on-line UPS system for low power applications," in *Proc. IEEE APEC'08*, 2008, pp.1296 – 1302. 1983

